12th International Conference on Electrical, Electronics and Computer Engineering (IcETRAN), Čačak, 9-12 June 2025

Application of Machine Learning in Predicting the Force of Radial Passive Magnetic Bearing

Isidora Jovanović
Dept. of Theoretical Electrical Engineering
University of Niš, Faculty of Electronic Engineering
Niš, Serbia
isidora.jovanovic@elfak.ni.ac.rs
0009-0000-1150-6611

Natalija Ivković
Dept. of Theoretical Electrical Engineering
University of Niš, Faculty of Electronic Engineering
Niš, Serbia
natalija.ivkovic@elfak.ni.ac.rs
0009-0006-5218-4544

Ana Vučković
Dept. of Theoretical Electrical Engineering
University of Niš, Faculty of Electronic Engineering
Niš, Serbia
ana.vuckovic@elfak.ni.ac.rs
0000-0002-9794-4248

Mirjana Perić
Dept. of Theoretical Electrical Engineering
University of Niš, Faculty of Electronic Engineering
Niš, Serbia
mirjana.peric@elfak.ni.ac.rs
0000-0001-8670-2254

Nebojša Raičević
Dept. of Theoretical Electrical Engineering
University of Niš, Faculty of Electronic Engineering
Niš, Serbia
nebojsa.raicevic@elfak.ni.ac.rs
0000-0003-0498-2307

***Abstract*—This paper investigates the application of machine learning methods for predicting the interaction force between ring-shaped permanent magnets in radial passive magnetic bearings. A semi-numerical approach based on the application of fictitious magnetic charges is used to produce datasets for training three different models: Random Forest, Polynomial regression, and Kernel Ridge regression. The findings highlight the potential of machine learning as an effective alternative to traditional force calculation methods.**

Keywords—machine learning, magnetic charges, magnetic force, passive magnetic bearings, permanent magnet

I. Introduction

Ring-shaped permanent magnets play a vital role across various industrial, technological, and medical applications. They are utilized in electric motors and generators for efficient power generation and transmission, in sensors and encoders for precise position and speed measurement, and also in audio devices, like speakers and microphones, to enable the conversion between electrical signals and sound. Their capability to generate stable and strong magnetic fields makes them essential for applications requiring high precision and reliability. The performance of ring-shaped permanent magnets depends on their material properties, magnetization, and dimensions. A notable application is in magnetic bearings, which utilize permanent magnets to achieve contactless suspension. These bearings can operate in axial [1] or radial [2] configurations, enabling precise position control and axis centering. A comprehensive understanding of magnetic field and magnetic force interactions in such systems is essential for ensuring their stability and reliability [3].

Common models used for determining the forces between permanent magnets include Ampere's current model [4] and the Coulombian approach [5,6]. Several studies have previously calculated levitation forces for permanent magnets, showcasing the versatility and importance of accurate analysis in these applications. However, these methods are mostly suited to specific geometries, particularly block [7-9] and cylindrical structures [10-12], limiting their applicability in more complex scenarios with alternative geometries. While they can be effective in simple cases, these methods might not provide comprehensive solutions for all types of magnetic configurations.

Traditional approaches for calculating the force between two magnets often involve complex mathematical formulations and computationally intensive procedures, with their complexity varying based on the magnets' geometry, material properties, and magnetization characteristics. These challenges make it increasingly beneficial to explore alternative methods for solving such problems. Machine learning presents a promising approach by leveraging data-driven models to solve various electromagnetic problems, potentially reducing computational cost while maintaining accuracy [13]. With the use of advanced learning algorithms, predictive models can be created to efficiently estimate magnetic forces between permanent magnets in various configurations, such as cylindrical [14] or block magnets [15], offering a novel approach to this complex problem.

The aim of this paper is to utilize machine learning for predicting the force between two ring magnets within a passive magnetic bearing and to compare the results and efficiency with those obtained using a semi-numerical approach based on fictitious magnetic charges. For the purpose of force prediction, three machine learning models are utilized: Random Forest, Polynomial regression, and Kernel Ridge regression and are trained on datasets generated through a semi-numerical approach.

II. Model and Semi-Numerical Analysis

The problem examined in this paper concerns a passive magnetic bearing with radial magnetization suspended in air, Fig. 1, and interaction force between its permanent magnets.

In Fig. 1, the inner radii of the upper and lower ring permanent magnets are denoted by *a* and *c*, while the outer radii

ISBN 978-86-6200-031-6 ©2025 AM & ETRAN

https://doi.org/10.69994/12Ic25003

are denoted by b and d. $\boldsymbol{M}_1$ and $\boldsymbol{M}_2$ represent magnetization vectors.

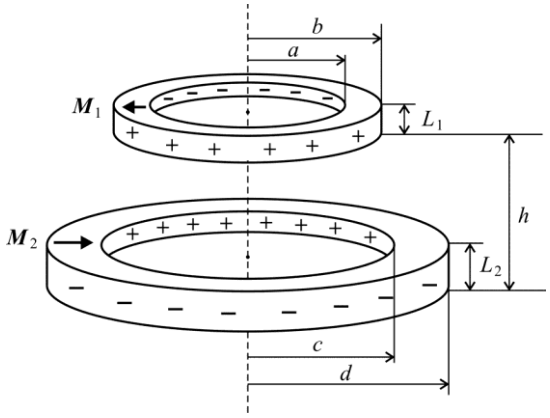

Fig. 1. Radial passive magnetic bearing.

The problem of determining the interactive force between two permanent magnets within a magnetic bearing has been addressed through the application of a discretization model derived from the application of fictitious magnetic charges [16]. Specifically, the entire system is divided into thin rings, each containing a specific amount of magnetic charge, which arises from both fictitious surface and volume magnetic charges.

As shown in [16] both magnets must satisfy the boundary condition for surface magnetization charge density, $\eta_{\mathrm{m}} = \hat{n} \cdot \boldsymbol{M}$, and based on the fulfillment of this boundary condition, the following expressions for fictitious surface magnetic charges are derived:

$$\eta_{\mathrm{m1}} = \hat{n}_1 \cdot \boldsymbol{M}_1 = -M_1, \tag{1}$$

$$\eta_{\mathrm{m2}} = \hat{n}_2 \cdot \boldsymbol{M}_1 = M_1, \tag{2}$$

$$\eta_{\mathrm{m3}} = \hat{n}_3 \cdot \boldsymbol{M}_2 = M_2, \tag{3}$$

$$\eta_{\mathrm{m4}} = \hat{n}_4 \cdot \boldsymbol{M}_2 = -M_2, \tag{4}$$

where $\hat{n}_1$, $\hat{n}_2$, $\hat{n}_3$ and $\hat{n}_4$ denote the unit vectors normal to the surface. Fictitious volume magnetic charges exist within both permanent magnets that form the magnetic bearing, and they must satisfy condition $\rho_{\mathrm{m}} = -\mathrm{div}\boldsymbol{M} = -\dfrac{M}{r}$. It is applied to both magnets, yielding the following relations:

$$\rho_{\mathrm{m1}} = -\mathrm{div}\boldsymbol{M}_1 = -\frac{M_1}{r}, \tag{5}$$

$$\rho_{\mathrm{m2}} = -\mathrm{div}\boldsymbol{M}_2 = \frac{M_2}{r}. \tag{6}$$

Therefore, the magnetic bearing model can also be represented as a system of fictitious surface and volume magnetic charges, as it is illustrated in Fig. 2.

Considering the geometry of the ring-shaped permanent magnet, Fig. 2, key parameters can be identified and specified for the parts of both the inner and outer covers of the upper and lower magnets.

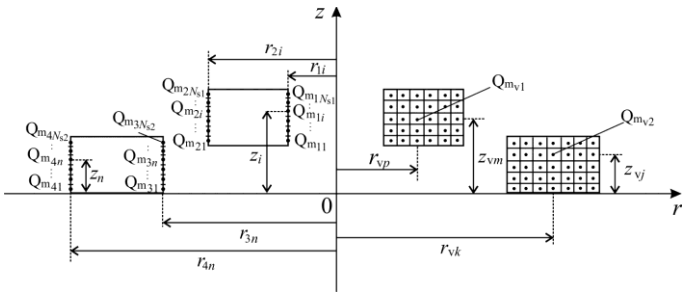

Fig. 2. Discretization model.

The parameters for the cover segments of the upper magnet are:

$$z_i = h + \frac{2i-1}{2N_{\mathrm{s1}}} L_1,\ i = 1, 2, ..., N_{\mathrm{s1}}, \tag{7}$$

$$r_{1i} = a,\ i = 1, 2, ..., N_{\mathrm{s1}}, \tag{8}$$

$$r_{2i} = b,\ i = 1, 2, ..., N_{\mathrm{s1}}, \tag{9}$$

and magnetic charges of the loops in upper magnet's inner and outer cover are:

$$Q_{\mathrm{m1}i} = -M_1 2\pi a \frac{L_1}{N_{\mathrm{s1}}},\ i = 1, 2, ..., N_{\mathrm{s1}}, \tag{10}$$

$$Q_{\mathrm{m2}i} = M_1 2\pi b \frac{L_1}{N_{\mathrm{s1}}},\ i = 1, 2, ..., N_{\mathrm{s1}}. \tag{11}$$

The parameters of the lower magnet are given by the following expressions:

$$z_n = \frac{2n-1}{2N_{\mathrm{s2}}} L_2,\ n = 1, 2, ..., N_{\mathrm{s2}}, \tag{12}$$

$$r_{3n} = c,\ n = 1, 2, ..., N_{\mathrm{s2}}, \tag{13}$$

$$r_{4n} = d,\ n = 1, 2, ..., N_{\mathrm{s2}}, \tag{14}$$

$$Q_{\mathrm{m3}n} = M_2 2\pi c \frac{L_2}{N_{\mathrm{s2}}},\ n = 1, 2, ..., N_{\mathrm{s2}}, \tag{15}$$

$$Q_{\mathrm{m4}n} = -M_2 2\pi d \frac{L_2}{N_{\mathrm{s2}}},\ n = 1, 2, ..., N_{\mathrm{s2}}, \tag{16}$$

where $Q_{\mathrm{m3}n}$ and $Q_{\mathrm{m4}n}$ represent magnetic charges of the inner and outer cover loops. Numbers of cover segments for upper and lower permanent magnet are denoted by N_{s1} and N_{s2}.

The fictitious volume magnetic charges are distributed throughout the entire volume of both the upper and lower

magnets in the form of circular loops. The parameters of these loops, as well as their magnetic charges are given below in (17)-(19) for the upper permanent magnet and in (20)-(22) for the lower permanent magnet.

$$z_{\mathrm{v}m} = h + \frac{2m-1}{2N_{\mathrm{v}1}} L_1,\ m = 1,2,...,N_{\mathrm{v}1}, \tag{17}$$

$$r_{\mathrm{v}p} = a + \frac{2p-1}{2N_{\mathrm{v}2}}(b-a),\ p = 1,2,...,N_{\mathrm{v}2}, \tag{18}$$

$$Q_{\mathrm{mv}1} = Q_{\mathrm{mv}i} = -M_1 2\pi L_1 \frac{b-a}{N_{\mathrm{v}1}N_{\mathrm{v}2}},\ i = 1,2,...,N_{\mathrm{v}1}N_{\mathrm{v}2}, \tag{19}$$

$$z_{\mathrm{v}j} = \frac{2j-1}{2N_{\mathrm{v}3}} L_2,\ j = 1,2,...,N_{\mathrm{v}3}, \tag{20}$$

$$r_{\mathrm{v}k} = c + \frac{2k-1}{2N_{\mathrm{v}4}}(d-c),\ k = 1,2,...,N_{\mathrm{v}4}, \tag{21}$$

$$Q_{\mathrm{mv}2} = Q_{\mathrm{mv}n} = M_2 2\pi L_2 \frac{d-c}{N_{\mathrm{v}3}N_{\mathrm{v}4}},\ n = 1,2,...,N_{\mathrm{v}3}N_{\mathrm{v}4}, \tag{22}$$

where $N_{\mathrm{v}1}N_{\mathrm{v}2}$ and $N_{\mathrm{v}3}N_{\mathrm{v}4}$ represent the number of loops in upper and lower permanent magnet, respectively. Using the procedure described in [16], where all mutual influences of the fictitious magnetic loads are summed, the following expression is obtained for the interactive force between the two permanent magnets that form the magnetic bearing:

$$\begin{aligned}
F_z = \frac{\mu_0}{2\pi}\Bigg(& \sum_{i=1}^{N_{\mathrm{s}1}}\sum_{n=1}^{N_{\mathrm{s}2}}\Big(Q_{\mathrm{m}1i}Q_{\mathrm{m}3n}F_{z_{\mathrm{p}}}(r_{3n}, r_{1i}, z_n, z_i) + \\
& + Q_{\mathrm{m}2i}Q_{\mathrm{m}3n}F_{z_{\mathrm{p}}}(r_{3n}, r_{2i}, z_n, z_i) + \\
& + Q_{\mathrm{m}1i}Q_{\mathrm{m}4n}F_{z_{\mathrm{p}}}(r_{4n}, r_{1i}, z_n, z_i) + \\
& + Q_{\mathrm{m}2i}Q_{\mathrm{m}4n}F_{z_{\mathrm{p}}}(r_{4n}, r_{2i}, z_n, z_i)\Big) + \\
& + \sum_{n=1}^{N_{\mathrm{s}2}}\sum_{m=1}^{N_{\mathrm{v}1}}\sum_{p=1}^{N_{\mathrm{v}2}}\Big(Q_{\mathrm{mv}1}Q_{\mathrm{m}3n}F_{z_{\mathrm{p}}}(r_{3n}, r_{\mathrm{v}p}, z_n, z_{\mathrm{v}m}) + \\
& + Q_{\mathrm{mv}1}Q_{\mathrm{m}4n}F_{z_{\mathrm{p}}}(r_{4n}, r_{\mathrm{v}p}, z_n, z_{\mathrm{v}m})\Big) + \\
& + \sum_{i=1}^{N_{\mathrm{s}1}}\sum_{j=1}^{N_{\mathrm{v}3}}\sum_{k=1}^{N_{\mathrm{v}4}}\Big(Q_{\mathrm{mv}2}Q_{\mathrm{m}1i}F_{z_{\mathrm{p}}}(r_{\mathrm{v}k}, r_{1i}, z_{\mathrm{v}j}, z_i) + \\
& + Q_{\mathrm{mv}2}Q_{\mathrm{m}2i}F_{z_{\mathrm{p}}}(r_{\mathrm{v}k}, r_{2i}, z_{\mathrm{v}j}, z_i)\Big) + \\
& + \sum_{m=1}^{N_{\mathrm{v}1}}\sum_{p=1}^{N_{\mathrm{v}2}}\sum_{j=1}^{N_{\mathrm{v}3}}\sum_{k=1}^{N_{\mathrm{v}4}} Q_{\mathrm{mv}2}Q_{\mathrm{mv}1}F_{z_{\mathrm{p}}}(r_{\mathrm{v}k}, r_{\mathrm{v}p}, z_{\mathrm{v}j}, z_{\mathrm{v}m})\Bigg),
\end{aligned} \tag{23}$$

where $F_{z_{\mathrm{p}}}(r_0, r_m, z_0, z_m)$ is determined as:

$$F_{z_{\mathrm{p}}}(r_0, r_m, z_0, z_m) = \frac{(z_m - z_0)E\left(\frac{\pi}{2}, k_0\right)}{\left((r_m - r_0)^2 + (z_m - z_0)^2\right)\sqrt{(r_m + r_0)^2 + (z_m - z_0)^2}} \tag{24}$$

In (24) the complete elliptic integral of the second kind is denoted by $E\left(\frac{\pi}{2}, k_0\right)$, while its module is defined as $k_0^2 = \frac{4r_m r_0}{(r_m + r_0)^2 + (z_m - z_0)^2}$. For the purpose of creating datasets for training the machine learning models authors used (23).

III. MACHINE LEARNING MODELS

For estimating the magnetic interaction force based on varying numbers of input parameters, three different machine learning methods implemented in Python using the Scikit-learn library are employed: Random Forest (RF), Polynomial regression (PR) and Kernel Ridge regression (KRR).

Random Forest [17] is a machine learning method that combines the predictions of multiple decision trees to obtain a final forecast. Its advantage over individual decision trees is the correction of overfitting. This method can solve both classification and regression problems. Some of its benefits, in addition to reducing overfitting, include high accuracy and the ability to handle large datasets. Since it can process nonlinear and complex data, it is one of the most commonly used machine learning methods.

While Linear regression represents a linear relationship between predictions and input data, Polynomial regression [18] is a technique that extends linear regression to model a nonlinear relationship. As a result, Polynomial regression is utilized to approximate complex functions and is more flexible than linear regression.

Kernel Ridge [19] regression combines Ridge regression with kernel functions. Ridge regression is an extension of Linear regression that includes L2 regularization, meaning it only models linear relationships. The key to Kernel Ridge regression is the transformation of the input data. Instead of directly using the input data, as Linear or Ridge regression does, KRR transforms it into a high-dimensional space using a kernel function. This is why this method represents a good solution for modeling nonlinear relationships between the input data and the predictions.

IV. NUMERICAL RESULTS

In this part of the paper, the obtained normalized force prediction from three different machine learning models (RF, PR and KRR) are presented and compared. Normalized force is calculated using the following expression:

$$F_z^{\mathrm{nor}} = \frac{F_z}{\mu_0 M^2 L_2^2}, \tag{25}$$

where $M_1 = M_2 = M$.

First, the simplest example was considered, in which the parameter h/L_2 is variable, and the parameters a/L_2, b/L_2,

c/L_2 and d/L_2 are fixed at $a/L_2 = 2.4$, $b/L_2 = 4$, $c/L_2 = 4.5$ and $d/L_2 = 5.6$. The dataset that contains 401 data points is used to train the machine learning models. The number of samples in datasets used for training the models is determined based on the complexity of the problem and the authors' previous experience. Table I presents the predictions obtained using the Kernel Ridge regression method with regularization parameter, $\alpha = 0.001$, and kernel coefficient, $\gamma = 12.9154966501488$. Table II shows the results for Random Forest with 100 trees, and Table III displays the predictions for Polynomial regression of degree 7. The related errors are also presented in the tables below.

TABLE I. KERNEL RIDGE REGRESSION PREDICTIONS FOR VARIABLE PARAMETER h/L_2

h/L_2	F_z^{nor}	$F_z^{nor}(KRR)$	δ [%]
-1.628	-0.63181	-0.63182	0.0018
0.314	1.32072	1.32069	0.0024
1.273	1.19384	1.19381	0.0021
-0.869	-1.87525	-1.87521	0.0022

TABLE II. RANDOM FOREST PREDICTIONS FOR VARIABLE PARAMETER h/L_2

h/L_2	F_z^{nor}	$F_z^{nor}(RF)$	δ [%]
-1.628	-0.63181	-0.62693	0.772
0.314	1.32072	1.32612	0.409
1.273	1.19384	1.18927	0.383
-0.869	-1.87525	-1.87587	0.033

TABLE III. POLYNOMIAL REGRESSION PREDICTIONS FOR VARIABLE PARAMETER h/L_2

h/L_2	F_z^{nor}	$F_z^{nor}(PR)$	δ [%]
-1.628	-0.63181	-0.61478	2.696
0.314	1.32072	1.26183	4.459
1.273	1.19384	1.17369	1.688
-0.869	-1.87525	-1.92271	2.531

It can be concluded from the presented values that the Kernel Ridge regression method provides exceptionally good predictions, also Random Forest does not lag far behind. Therefore, the idea is to reduce the training set to solve the problem more optimally. Instead of a training set with 401 data points, a training set with 41 data points is used for the same variable range. The predictions, obtained using the new reduced training set, are presented in Table IV for KRR, Table V for RF, and Table VI for PR.

TABLE IV. KERNEL RIDGE REGRESSION PREDICTIONS WITH SMALLER TRAINING DATASET FOR VARIABLE PARAMETER h/L_2

h/L_2	F_z^{nor}	$F_z^{nor}(KRR)$	δ [%]
-0.43	-1.64729	-1.64738	0.0054
1.59	0.68144	0.68162	0.0253
1.98	0.28410	0.28403	0.0247
0.32	1.34029	1.34016	0.0097

TABLE V. RANDOM FOREST PREDICTIONS WITH SMALLER TRAINING DATASET FOR VARIABLE PARAMETER h/L_2

h/L_2	F_z^{nor}	$F_z^{nor}(RF)$	δ [%]
-0.43	-1.64729	-1.61998	1.658
1.59	0.68144	0.71886	5.490
1.98	0.28410	0.31210	9.859
0.32	1.34029	1.25822	6.123

TABLE VI. POLYNOMIAL REGRESSION PREDICTIONS WITH SMALLER TRAINING DATASET FOR VARIABLE PARAMETER h/L_2

h/L_2	F_z^{nor}	$F_z^{nor}(PR)$	δ [%]
-0.43	-1.64729	-1.57967	4.105
1.59	0.68144	0.64525	5.311
1.98	0.28410	0.26677	6.098
0.32	1.34029	1.27761	4.677

The results for KRR remain exceptionally good, even though the training dataset has been reduced by almost 10 times, while the error for the other two machine learning methods has increased. The time required to obtain a prediction is less than a second. Since Kernel Ridge regression delivers outstanding results even with the reduced dataset, it was decided to use only this method for prediction in further work and to gradually increase the number of variables. Fig. 3 shows the overlap between the actual values of the normalized force and the predictions for the KRR model.

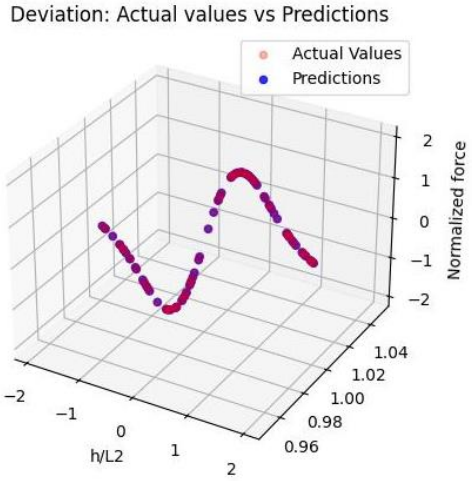

Fig. 3. Matches between predicted outputs and actual outputs.

The Kernel Ridge regression model was also trained with a dataset that consists of around 6600 data points, where the parameters a/L_2, b/L_2 and h/L_2 are variable, while the remaining parameters are fixed, specifically $c/L_2 = 5.5$ and $d/L_2 = 7$. The Kernel Ridge regression parameters are $\alpha = 0.001$ and $\gamma = 12.9154966501488$. The obtained predictions along with the corresponding errors can be seen in Table VII.

TABLE VII. KERNEL RIDGE REGRESSION OUTPUTS FOR FIXED PARAMETERS $c/L_2 = 5.5$ AND $d/L_2 = 7$

a/L_2	b/L_2	h/L_2	F_z^{nor}	$F_z^{nor}(KRR)$	δ [%]
2.15	3.12	-1.56	-0.15047	-0.14984	0.422
2.87	3.65	-1.12	-0.26379	-0.26405	0.099
3.64	3.94	-0.69	-0.17970	-0.17942	0.155
3.21	4.26	0.48	0.51787	0.51778	0.016
2.49	4.58	0.97	1.39551	1.38947	0.433

The previous table shows that the errors are satisfactory. The program's prediction time using the already trained model is around 0.4 seconds. The semi-numerical method required approximately 0.09 seconds to obtain the solution. Fig. 4 illustrates the deviation between the actual values and the predictions for this case of fixed and variable parameters. This visualization provides insight into the model's accuracy, the closer the points are to the diagonal line, the closer the predictions are to the actual values.

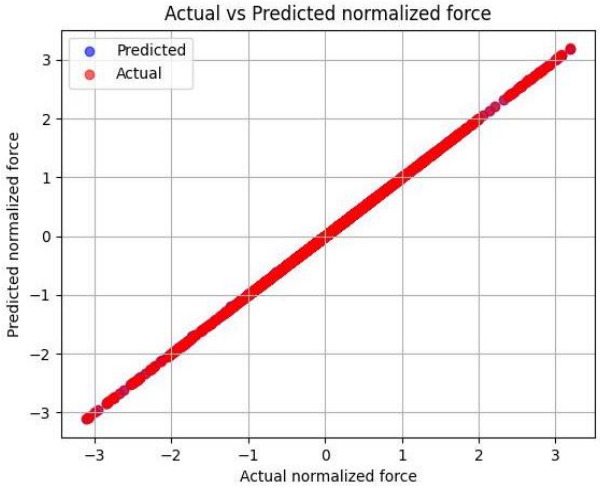

Fig. 4. Comparison of actual and predicted normalized force values for fixed parameters c/L_2 and d/L_2 .

The next example that is processed is for the same number of variable parameters, but now they are c/L_2 , d/L_2 and h/L_2 , while the fixed parameters are $a/L_2 = 2.2$ and $b/L_2 = 3.3$, while regression parameters remain the same as those used in prediction shown in Table VII. The obtained results are presented in Table VIII.

TABLE VIII. KERNEL RIDGE REGRESSION PREDICTIONS FOR FIXED PARAMETERS $a/L_2 = 2.2$ AND $b/L_2 = 3.3$

c/L_2	d/L_2	h/L_2	F_z^{nor}	$F_z^{nor}(KRR)$	δ [%]
3.78	5.61	-0.81	-1.72209	-1.72021	0.109
3.96	6.42	1.62	0.66796	0.66833	0.055
4.21	7.29	-1.54	-0.69918	-0.69874	0.062
4.64	6.93	0.49	0.39611	0.39675	0.160
5.32	7.18	-0.22	-0.07534	-0.07534	0.006

As can be seen, the errors are satisfactory in this case as well. A dataset with 7600 data points is used to train the model, and the prediction time is approximately 0.3 seconds, while obtaining the result using the semi-numerical method took around 0.13 seconds.

The most complex issue explored in this paper involves a situation where the parameters a/L_2 , b/L_2 , c/L_2 , and d/L_2 are variable, while only the parameter h/L_2 is fixed at $h/L_2 = 1$. A total of approximately 5900 data points were used to train the model in this case, and the results obtained from testing this model are presented in Table IX. The Kernel Ridge regression parameters used in this case are $\alpha = 0.001$ and $\gamma = 0.5994842503189$.

TABLE IX. RESULTS OF KERNEL RIDGE REGRESSION FOR FIXED PARAMETER $h/L_2 = 1$

a/L_2	b/L_2	c/L_2	d/L_2	F_z^{nor}	$F_z^{nor}(KRR)$	δ [%]
2.35	3.7	5.75	7.2	0.27074	0.27049	0.094
2.56	4.2	5.34	7.3	1.00725	1.00743	0.018
2.28	3.68	5.92	7.46	0.23196	0.23130	0.287
2.17	4.48	5.24	6.61	1.61688	1.59977	1.058
2.89	3.91	5.13	6.97	0.70426	0.70562	0.194

The program's prediction time is 0.38 seconds and the solution is computed using the semi-numerical method in roughly 0.15 seconds. It is concluded that the errors are within an acceptable range in this case as well. Fig. 5 shows the overlap of the outputs, which directly demonstrates the model's accuracy.

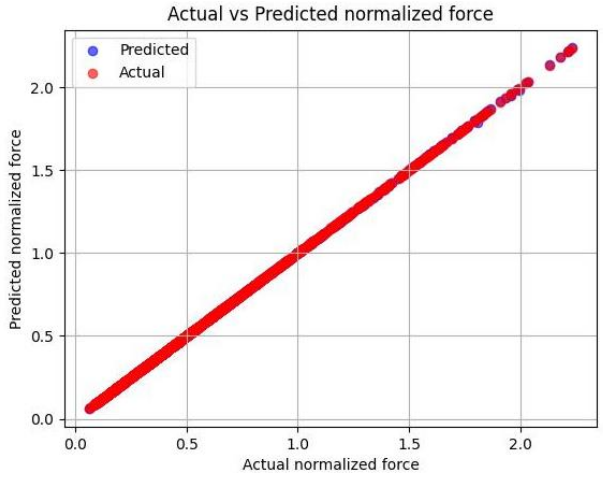

Fig. 5. Comparison of actual and predicted normalized force values for fixed parameter h/L_2 .

It is obvious that in every analyzed case, the errors were satisfactory, indicating that machine learning, specifically Kernel Ridge regression, can be successfully applied to calculate the normalized force between two permanent ring magnets with radial magnetization.

CONCLUSION

This study examined the problem of calculating the normalized force between two permanent ring magnets with radial magnetization. The results indicate that machine learning can be successfully applied to this problem, and among all the tested methods, Kernel Ridge regression yields the best results. Polynomial regression did not provide good predictions in any instance, whereas the random forest produced satisfactory

predictions when the parameter h/L_2 was changed. However, it required ten times more training data and, consequently, more time for prediction. Furthermore, even with a significantly reduced training dataset, KRR maintains high accuracy, making it a practical and efficient approach for this type of calculation. These findings show how machine learning, in particular KRR, can be used to solve magnetostatic issues. Although the computation time using the semi-numerical method is shorter, the time required to obtain a prediction from the machine learning model is also below one second, which represents a satisfactory result. A significant advantage of applying machine learning to magnetostatic problems is the ability to generate training datasets not only through computational methods but also through direct measurements, further enhancing the model applicability and accuracy.

ACKNOWLEDGMENT

This work has been supported by the Ministry of Science, Technological Development and Innovation of the Republic of Serbia [Grant Number: 451-03-137/2025-03/ 200102].

REFERENCES

[1] R. Ravaud, G. Lemarquand and V. Lemarquand, "Force and Stiffness of Passive Magnetic Bearings Using Permanent Magnets. Part 1: Axial Magnetization," in IEEE Transactions on Magnetics, vol. 45, no. 7, July 2009, pp. 2996-3002.

[2] R. Ravaud, G. Lemarquand and V. Lemarquand, "Force and Stiffness of Passive Magnetic Bearings Using Permanent Magnets. Part 2: Radial Magnetization," in IEEE Transactions on Magnetics, vol. 45, no. 9, Sept. 2009, pp. 3334-3342.

[3] K. D. Bachovchin, J. F. Hoburg and R. F. Post, "Magnetic Fields and Forces in Permanent Magnet Levitated Bearings," in IEEE Transactions on Magnetics, vol. 48, no. 7, July 2012, pp. 2112-2120.

[4] A. N. Vučković, S. S. Ilić and S. R. Aleksić, "Interaction magnetic force calculation of ring permanent magnets using Ampere's microscopic surface currents and discretization technique". Electromagnetics, Vol. 32, No. 2, 2012, pp. 117-134.

[5] H. L. Rakotoarison, J.P. Yonnet and B. Delinchant, "Using Coulombian approach for modeling scalar potential and magnetic field of a permanent magnet with radial polarization", IEEE Transactions on magnetics, Vol.43, 2007, pp. 1261-1264.

[6] R. Ravaud, G. Lemarquand, V. Lemarquand and C. Depollier, "Analytical Calculation of the Magnetic Field Created by Permanent-Magnet Rings", IEEE Transactions on magnetics, 44, No. 8, 2008, pp. 1982-1989.

[7] M. Beleggia, D. Vokoun, M. D. Graef; "Forces between a permanent magnet and a soft magnetic plate", IEEE Magnetic letters, Vol. 3, 2012.

[8] G. Akoun and J. P. Yonnet, "3D analytical calculation of the forces exerted between two cuboidal magnets", IEEE Transactions on magnetics, Vol. 20, 1984, pp. 1962-1964.

[9] A. Vučković, M. Perić, S. Ilić, N. Raičević and D. Vučković, "Interaction magnetic force of cuboidal permanent magnet and soft magnetic bar using hybrid boundary element method", ACES journal, Vol. 36, No. 11, 2021, pp. 1492-1498.

[10] W. Yang, G. Zhou, K. Gong and Y. Li, "The numeric calculation for cylindrical magnet's magnetic flux intensity", International journal of applied electromagnetics and mechanics, IOS Press, Vol. 40, No. 3, 2012, pp. 227-235.

[11] E. P. Furlani, S. Reznik and A. Kroll, "A three-dimensional field solution for radially polarized cylinders", IEEE Transactions on magnetics, Vol. 31, 1995, pp. 844–851.

[12] W. S. Robertson, B. S. Cazzolato and A. C. Zander, "A Simplified force equation for coaxial cylindrical magnets and thin coils", IEEE Transactions on magnetics, Vol. 47, No. 8, 2011, pp. 2045–2049.

[13] D. Olćan and D. Ninković, "Machine learning in applied electromagnetics", 11th Int. Conf. on Electrical, Electronics and Computer Engineering (IcETRAN), Niš, June 3-6, 2024, pp. 23-26.

[14] N. Ivković, A. Vučković, M. Perić and D. Vučković, "Machine learning application in cylindrical permanent magnet force calculation", 16th Int. Conference on Applied Electromagnetics – IIEC 2023, Faculty of Electronic Engineering of Niš, Niš, Serbia, August 28-30, 2023, CD-proceedings, pp. 89-92.

[15] A. Stojanović, D. Vučković, M. Stanković and A. Vučković, "Machine learning application in permanent magnet force calculation", 13th Int. Conference on Applied Electromagnetics – IIEC 2017, Faculty of Electronic Engineering of Niš, Niš, Serbia, 2017, CD-proceedings.

[16] A. Vučković, N. Raicevic, S. Ilic and S. Aleksic, "Interaction magnetic force calculation of radial passive magnetic bearing using magnetization charges and discretization technique", International Journal of Applied Electromagnetics and Mechanics, 43, 2013, pp. 311-323.

[17] Biau G., "Analysis of a random forests model", The Journal of Machine Learning Research, Vol. 13 No. 1, pp. 1063-1095, 2012.

[18] Ostertagová E., "Modelling using polynomial regression" Procedia engineering, Vol. 48, 2012, pp. 500-506.

[19] Saunders C., Gammerman A. and Vovk V, "Ridge regression learning algorithm in dual variables", 15th International Conference on Machine Learning, 1998, ICML '98.